J|A|C|S ARTICLES

Published on Web 05/04/2009

# Sulfur versus Oxygen Reactivity of Organic Molecules at the Ge(100)-2×1 Surface

Jessica S. Kachian and Stacey F. Bent*

*Department of Chemical Engineering, Stanford University, Stanford, California 94305*

Received October 13, 2008; E-mail: sbent@stanford.edu

***Abstract:*** The adsorption behavior of sulfur- versus oxygen-containing organic molecules, including ethanol, ethanethiol, diethyl ether, and diethyl sulfide, at the Ge(100)-2×1 surface was investigated using a combination of multiple internal reflection infrared (MIR-IR) spectroscopy and density functional theory (DFT). The results show that ethanol and ethanethiol both adsorb via Ch−H dissociation at 310 K, where Ch (chalcogen) is either S or O. DFT calculations indicate that S−H dissociation is both kinetically and thermodynamically favored over O−H dissociation. IR spectra of diethyl ether and diethyl sulfide reveal that both molecules adsorb via dative bonding through the heteroatom for temperatures up to approximately 255 and 335 K, respectively, and reversibly desorb at higher temperatures. From these desorption temperatures, the S−Ge dative bond of a sulfide is calculated to be 5.9 kcal/mol stronger than the O−Ge dative bond of an ether, a trend consistent with results from DFT calculations. Moreover, for all of the molecules studied, S−Ge dative bonds are found to be stronger than O−Ge dative bonds, with the magnitude of the difference increasing with substitution of bulkier groups on the Ch atom of the adsorbate. Calculations on diethyl selenide show that the Se−Ge dative bond is slightly stronger than the S−Ge dative bond.

## 1. Introduction

With the semiconductor industry fast approaching the limits of traditional device scaling, current research has focused on alternative materials for metal-oxide-semiconductor field-effect transistors. A substantial amount of work has focused on replacing the silicon transistor channel with a higher mobility material. Germanium, also a Group IV semiconductor, has attracted considerable interest, since it offers bulk electron and hole mobilities three and four times higher than those for silicon at room temperature, respectively.[1] However, unlike silicon's native oxide, germanium oxides are thermally unstable and form poor electrical-quality interfaces with the underlying germanium.[2,3] Consequently, an alternative passivating layer is required for the germanium surface.

Thus far, sulfur has been shown to be one of the best passivants of the germanium surface.[4] Sulfur passivation of the germanium surface has been achieved with both solution and vacuum deposition techniques and with a variety of sulfur sources and germanium crystal orientations. Weser et al.[5] achieved a 1-ML saturated S/Ge(100)-1×1 surface via chemisorption of elemental sulfur on the Ge(100)-2×1 surface under ultrahigh vacuum (UHV) conditions. Anderson et al.[6] treated a hydrogen-terminated Ge(100) surface with an aqueous solution of $(NH_4)_2S$ to yield an S-passivated Ge(100)-1×1 surface with a 1 ML coverage of bridge-bonded sulfur atoms and thermal stability to 475 K. Recently, Frank et al.[7] used Anderson's deposition technique and demonstrated that sulfur passivation is substantially preserved during high-$\kappa$ dielectric growth and results in improved electrical properties of $HfO_2$/Ge stacks. Yet another sulfur passivation method employs the exposure of an alkanethiol solution to the hydrogen-terminated Ge(111) surface, yielding a thiolated Ge(111) surface, which couples the strength of the S−Ge bond with the protection afforded by alkyl chain packing.[8,9]

In order to understand sulfidation of the germanium surface and its possible superiority to oxidation in passivating this surface, we have conducted a UHV study investigating reaction of the clean Ge(100)-2×1 surface with a range of sulfur-containing functional groups (thiol and sulfide) and their oxygen-containing counterparts (alcohol and ether).

Conducting the study in ultrahigh vacuum (UHV) isolates adsorbate interactions with a well-defined germanium surface. Upon proper preparation, Ge(100) and Si(100) surfaces undergo a 2×1 reconstruction, which entails the formation of tilted surface dimers possessing a strong $\sigma$ bond and a weak $\Pi$ bond.[10] The tilting of these dimers creates an uneven distribution of charge within the dimer, resulting in an electron-rich, nucleophilic "up" atom and an electron-deficient, electrophilic "down"

(1) Maeda, T.; Takagi, S.; Ohnishi, T.; Lippmaa, M. *Mater. Sci. Semicond. Process.* **2006**, *9* (4−5), 706.
(2) Kingston, R. H. *J. Appl. Phys.* **1956**, *27* (2), 101.
(3) Prabhakaran, K.; Ogino, T. *Surf. Sci.* **1995**, *325* (3), 263.
(4) Losutoff, P. W.; Bent, S. F. *Annu. Rev. Phys. Chem.* **2006**, *57*, 467.
(5) Weser, T.; Bogen, A.; Konrad, B.; Schnell, R. D.; Schug, C. A.; Moritz, W.; Steinmann, W. *Surf. Sci.* **1988**, *201* (1−2), 245.
(6) Anderson, G. W.; Hanf, M. C.; Norton, P. R.; Lu, Z. H.; Graham, M. J. *Appl. Phys. Lett.* **1995**, *66* (9), 1123.
(7) Frank, M. M.; Koester, S. J.; Copel, M.; Ott, J. A.; Paruchuri, V. K.; Shang, H. L.; Loesing, R. *Appl. Phys. Lett.* **2006**, *89* (11), 112905.
(8) Han, S. M.; Ashurst, W. R.; Carraro, C.; Maboudian, R. *J. Am. Chem. Soc.* **2001**, *123* (10), 2422.
(9) Kosuri, M. R.; Cone, R.; Li, Q. M.; Han, S. M.; Bunker, B. C.; Mayer, T. M. *Langmuir* **2004**, *20* (3), 835.
(10) Kubby, J. A.; Boland, J. J. *Surf. Sci. Rep.* **1996**, *26* (3−6), 61.

  

atom.[10] Consequently, the "up" and "down" atoms of a dimer can function as a Lewis base and acid, respectively.[11] This chemical description plays a central role in explaining how the clean Ge(100)-2×1 surface reacts with each of the molecules investigated in this study.

The set of adsorbates, examined with both experimental and theoretical methods, includes ethanethiol, ethanol, diethyl ether, and diethyl sulfide. In addition, diethyl selenide, which also contains a chalcogen atom, was investigated theoretically. Each of these molecules contains an electronegative atom with two lone pairs of electrons. Previous UHV investigations of Si(100)-2×1 and Ge(100)-2×1 surface reaction with molecules also possessing the latter characteristic have shown that some adsorb via donation of a lone pair of electrons to the electron-deficient down atom of a Ge or Si dimer, thus forming a dative-bonded state.[12,13] Depending on the surface temperature and the chemical identities of the adsorbate and surface, this dative bond may exist as a stable adsorption state or as a precursor to subsequent surface reaction.[14,15] In the case of adsorption of ethanol on clean Si(100)-2×1, Silvestrelli[16] used ab initio quantum chemical simulations to show that ethanol undergoes O−H dissociation from a dative-bonded precursor state with an overall mechanism that is kinetically and thermodynamically favorable at room temperature. Others experimentally confirmed the room-temperature O−H dissociation of ethanol on the clean Si(100)-2×1 surface under UHV conditions using infrared absorption spectroscopy,[17] high-resolution synchrotron radiation photoemission,[18] and other experimental techniques.[19] In similar experiments with ethanethiol, Lai et al.[20] used X-ray photoelectron spectroscopy (XPS) and LEED to show that ethanethiol undergoes an analogous S−H dissociation on the clean Si(100)-2×1 at room temperature, leading to conservation of the 2×1 surface reconstruction.

In the present study, we use a combination of density functional theory (DFT) and multiple internal reflection-Fourier transform infrared (MIR-IR) spectroscopy to show that, like on silicon, ethanethiol and ethanol undergo Ch−H (where Ch refers to the chalcogen atom) dissociation on Ge(100)-2×1 at room temperature under UHV conditions to form thermodynamically stable products. However, the relative kinetics and thermodynamics of the Ch−H dissociation reactions are reversed on Ge(100)-2×1 compared to Si(100)-2×1. On Si(100)-2×1, molecularly adsorbed methanol undergoes O−H dissociation at 150 K,[21] whereas molecularly adsorbed methanethiol undergoes S−H dissociation at 170 K, [20] and our bond energy calculations indicate that O−H dissociation of ethanol is 3.7 kcal/mol more exothermic than S−H dissociation of ethanethiol on Si(100)-2×1. In contrast, the current results show that S−H dissociation is kinetically and thermodynamically more favorable than O−H dissociation on the Ge(100)-2×1 surface.

Diethyl ether and diethyl sulfide were studied to probe the strength of the S−Ge versus the O−Ge dative bond. These molecules were also compared theoretically with diethyl selenide. Each of these molecules adsorbs to the Ge(100)-2×1 surface via dative bonding through the Ch atom, and molecular desorption is expected upon heating. By measuring these desorption temperatures, the binding energy can be determined. Temperature-dependent IR spectra of diethyl sulfide and diethyl ether on Ge(100)-2×1 show that adsorbed diethyl sulfide and diethyl ether are observed only at temperatures up to 335 and 255 K, respectively, thus indicating the greater stability of the S−Ge dative bond over the O−Ge dative bond.

## 2. Experimental and Computational Details

Infrared spectroscopy experiments were completed under ultrahigh vacuum conditions (UHV) in a previously described reaction chamber[13] with a base pressure of less than $1\times10^{-10}$ Torr. The surface was prepared by $Ar^+$ sputtering at room temperature (20 mA emission current, 0.5 keV accelerating voltage, 7−8 $\mu$A sample current) for 20 min followed by annealing to 900 K and holding at this temperature for 5 min. The crystal used for infrared measurements is 19 × 14 × 1 mm with 45° beveled edges. Low-energy electron diffraction (LEED) confirmed that the proper surface reconstruction was achieved, and Auger electron spectroscopy (AES) verified that carbon, oxygen, and nitrogen surface concentrations were undetectable using this cleaning procedure. Infrared spectra were collected for a multiple internal reflection (MIR) geometry employing a BioRad FTS-60A Fourier transform infrared (FTIR) spectrometer equipped with a liquid nitrogen-cooled, narrow-band, mercury−cadmium−telluride (MCT) detector. The unpolarized beam from the FTIR spectrometer first entered the chamber through a $CaF_2$ viewport, was focused onto the beveled edge of a germanium MIR crystal (Umicore), and then exited through another $CaF_2$ viewport at a right angle to the first viewport. The beam path was purged by compressed air from which $H_2O$ and $CO_2$ had been filtered. The spectral range of the collected infrared data was limited by absorption by the $CaF_2$ windows, resulting in a low-frequency cutoff of ~1020 $cm^{-1}$. To record infrared spectra of unreacted molecules, multilayers were condensed on the surface of the sample at low temperature (<140 K). All spectra were corrected for baseline sloping via subtraction of linear functions between points enclosing regions with no spectral features.

Ethanethiol (97%, Sigma-Aldrich), ethanol (99.5%, Sigma-Aldrich), diethyl sulfide (99%, Sigma-Aldrich), and diethyl ether (99.9%, Sigma-Aldrich) are clear liquids at room temperature. Each liquid compound was purified by several freeze−pump−thaw cycles before exposure to the clean crystal surface. Exposure of a compound was accomplished by backfilling via a variable leak valve. Surface exposures are reported in Langmuir (1 L = $10^{-6}$ Torr*s), and pressures were not corrected for ionization gauge sensitivity. Following each surface exposure, the manifold lines were pumped to less than 20 mTorr before refilling for the following dose. An in situ quadrupole mass spectrometer confirmed the molecular identity and purity of each compound after introduction to the chamber.

Electronic structure calculations were completed with the Gaussian 03 software package[22] using Becke3 Lee−Yang−Parr (B3LYP) three-parameter density functional theory.[23] Previous studies of B3LYP indicate that it provides predictive results for similar

(11) Filler, M. A.; Bent, S. F. *Prog. Surf. Sci.* **2003**, *73* (1−3), 1.
(12) Wang, G. T.; Mui, C.; Musgrave, C. B.; Bent, S. F. *J. Phys. Chem. B* **2001**, *105* (16), 3295.
(13) Mui, C.; Han, J. H.; Wang, G. T.; Musgrave, C. B.; Bent, S. F. *J. Am. Chem. Soc.* **2002**, *124* (15), 4027.
(14) Wang, G. T.; Mui, C.; Tannaci, J. F.; Filler, M. A.; Musgrave, C. B.; Bent, S. F. *J. Phys. Chem. B* **2003**, *107* (21), 4982.
(15) Keung, A. J.; Filler, M. A.; Bent, S. F. *J. Phys. Chem. C* **2007**, *111* (1), 411.
(16) Silvestrelli, P. L. *Surf. Sci.* **2004**, *552* (1−3), 17.
(17) Eng, J.; Raghavachari, K.; Struck, L. M.; Chabal, Y. J.; Bent, B. E.; Flynn, G. W.; Christman, S. B.; Chaban, E. E.; Williams, G. P.; Radermacher, K.; Manti, S. *J. Chem. Phys.* **1997**, *106* (23), 9889.
(18) Casaletto, M. P.; Zanoni, R.; Carbone, M.; Piancastelli, M. N.; Aballe, L.; Weiss, K.; Horn, K. *Surf. Sci.* **2000**, *447* (1−3), 237.
(19) Zhang, L. H.; Carman, A. J.; Casey, S. M. *J. Phys. Chem. B* **2003**, *107* (33), 8424.
(20) Lai, Y. H.; Yeh, C. T.; Yeh, C. C.; Hung, W. H. *J. Phys. Chem. B* **2003**, *107* (35), 9351.
(21) Ehrley, W.; Butz, R.; Mantl, S. *Surf. Sci.* **1991**, *248* (1−2), 193.
(22) Frisch, M. J. T., et al. Gaussian 03, C.02; Gaussian, Inc., Wallingford, CT, 2004.
(23) Kohn, W.; Sham, L. J. *Phys. Rev.* **1965**, *140* (4A), A1133.

systems[14,24,25] and that it is in good agreement with experimental results when available.[14,19,26] A two-dimer $Ge_{15}H_{16}$ cluster in which the dimers are in the same row was used to model the Ge(100)-2×1 surface. This cluster facilitates modeling interdimer reactions while maintaining a lower computational cost than a cluster containing more dimers or two parallel dimers in adjacent rows. Dimer atoms and adsorbate atoms were modeled using the triple-ζ, 6-311++G(d,p) basis set. Subsurface Ge atoms were modeled using the LANL2DZ pseudopotential.[27−29] The use of the pseudopotential keeps calculations computationally manageable while producing sufficiently accurate results.[13]

In the calculations, subsurface germanium atoms were terminated with hydrogen atoms to approximate the presence of neighboring germanium atoms in a real crystal. These hydrogen atoms were modeled using a 6-31G(d) basis set. With respect to intradimer adducts, use of these terminal hydrogens allowed for full optimization of structures without geometric constraints. In modeling interdimer adducts, however, constraints were found to be necessary to achieve convergence. Consequently, in the interdimer calculations, optimization was performed by fixing the bottom two layers of Ge atoms in the ideal Ge crystal positions while allowing the top two layers of Ge atoms (including the dimer atoms) and the atoms of the chemisorbed adsorbate to relax. The hydrogen atoms that are used to fill the valence of the subsurface Ge atoms and form Ge−H bonds, which represent the truncated cluster bonds, are accordingly held rigid in the ideal crystal directions with a Ge−H bond length of 0.155 nm. In a few cases, intradimer adducts were also modeled using geometric constraints in order to allow a direct comparison with the analogous interdimer products. Such cases are identified in the paper.

Geometries of important local minima and transition states on each energy diagram were calculated. Local minima and transition states were verified with frequency calculations of the optimized structure using the same basis sets. All reported energies have been zero-point energy corrected. Calculated frequencies have been scaled by a factor of 0.96[30] for comparison with the experimental data. For the same purpose, simulated IR spectra were constructed using the calculated intensities, scaled calculated frequencies, and Lorentzian lineshapes with a full width at half-maximum (fwhm) of 4 $cm^{-1}$ to represent the IR bands.

Separate bond energy calculations with smaller surface clusters, also executed with the Gaussian 03 software package[22] using B3LYP DFT,[23] were carried out to determine covalent bond strengths. The ordinary covalent bond strength of the Se−Ge bond was calculated for the Ge surface. In addition, bond energy calculations were used to determine the relative energetics of the Ch−H dissociation reactions of ethanethiol and ethanol on the Ge and Si surfaces. For the determination of relative energetics, bonds broken or formed in *both* reactions on a particular surface were not considered, as the object of these calculations was to identify contributions to the *difference* in exothermicity of these reactions on a particular surface and then to compare the results across the Ge(100)-2×1 and Si(100)-2×1 surfaces. The $Ge(GeH_3)_3$ and $ChCH_2CH_3$ fragments and the $H_3CH_2CCh-Ge(GeH_3)_3$ molecule were used in calculating Ch−Ge bond energies. The $Si(SiH_3)_3$ and $ChCH_2CH_3$ fragments and the $H_3CH_2CCh-Si(SiH_3)_3$ molecule were used in calculating Ch−Si bond energies.The $ChCH_2CH_3$ fragment, the H atom, and the $H-ChCH_2CH_3$ molecule were used in calculating Ch−H bond energies. All atoms were modeled using the triple-ζ, 6-311++G(d,p) basis set. The reported bond energies have been zero-point energy corrected.

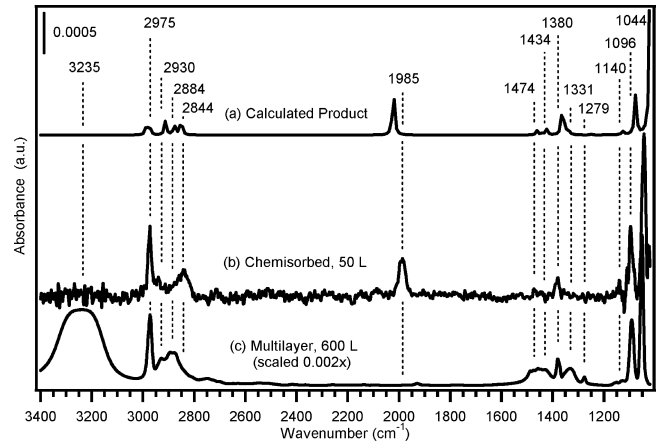


***Figure 1.*** (a) Calculated IR spectrum of the intradimer O−H dissociation product of ethanol across a Ge dimer on the two-dimer, intrarow $Ge_{15}H_{16}$ cluster. (b) An average of two IR spectra taken following saturation exposure of ethanol to Ge(100)-2×1 at 310 K. (c) An IR spectrum of a multilayer of ethanol on Ge(100)-2×1 taken at 140 K (intensity scaled). The peak labels correspond to chemisorbed and multilayer spectra. Geometry optimization of the product for which the IR spectrum displayed in part (a) was calculated was performed with no geometric constraints.

## 3. Results and Interpretation

**A. Ethanol versus Ethanethiol. 1. IR Analysis.** Figure 1 shows (a) the calculated IR spectrum for the O H−dissociated product, (b) an IR spectrum taken following saturation exposure of ethanol to Ge(100)-2×1 at 310 K, and (c) an IR spectrum of a multilayer of ethanol on Ge(100)-2×1 taken at 130 K, a temperature at which several layers of ethanol are condensed on the surface, thus isolating the solid-state modes of the adsorbate. The vibrational assignments for the major experimental peaks are found in the Supporting Information.

The multilayer spectrum in Figure 1c agrees well with previously reported IR spectra of ethanol in the solid phase[31,32] and of ethanol multilayers on Si(100).[17] A comparison of the multilayer spectrum to the chemisorbed spectrum in Figure 1b allows identification of modes that are gained or lost upon adsorption and, consequently, has implications toward adsorption structures. The peak at 1985 $cm^{-1}$, assigned to a Ge−H stretch, is one of the primary features gained upon adsorption. This mode implies that hydrogen has transferred from the molecule to the surface, corresponding to either C−H or O−H dissociation.

Previous studies of organic molecules on Ge(100)-2×1 have shown that C−H dissociation is kinetically prohibitive at room temperature with the exception of some molecules which adsorb via either electrophilic aromatic substitution or the "ene" reaction.[11] Consequently, C−H dissociation is deemed unlikely. On the other hand, the experimental data clearly point to the presence of O−H dissociation. The multilayer displays (1) a broad, intense peak at 3235 $cm^{-1}$, which is associated with O−H stretching, and (2) peaks at 1279, 1331, and 1434 $cm^{-1}$, which are associated with C−O−H bending. However, the chemisorbed spectrum lacks these features, indicating that O−H dissociation has occurred. This result is further supported by the close agreement between the chemisorbed spectrum and the IR spectrum calculated for the O−H dissociated product (Figure 1a). We note that the calculated spectrum for the interdimer

(24) Konecny, R.; Doren, D. J. *Surf. Sci.* **1998**, *417* (2−3), 169.
(25) Lu, X.; Lin, M. C. *Int. Rev. Phys. Chem.* **2002**, *21* (1), 137.
(26) Teplyakov, A. V.; Kong, M. J.; Bent, S. F. *J. Am. Chem. Soc.* **1997**, *119* (45), 11100.
(27) Hay, P. J.; Wadt, W. R. *J. Chem. Phys.* **1985**, *82* (1), 270.
(28) Wadt, W. R.; Hay, P. J. *J. Chem. Phys.* **1985**, *82* (1), 284.
(29) Hay, P. J.; Wadt, W. R. *J. Chem. Phys.* **1985**, *82* (1), 299.
(30) Scott, A. P.; Radom, L. *J. Phys. Chem.* **1996**, *100* (41), 16502.
(31) Perchard, J. P. J. *J. Chim. Phys. Phys.−Chim. Biol.* **1968**, *65* (10), 1856.
(32) Schriver, A.; Schriver-Mazzuoli, L.; Ehrenfreund, P.; d'Hendecourt, L. *Chem. Phys.* **2007**, *334* (1−3), 128.

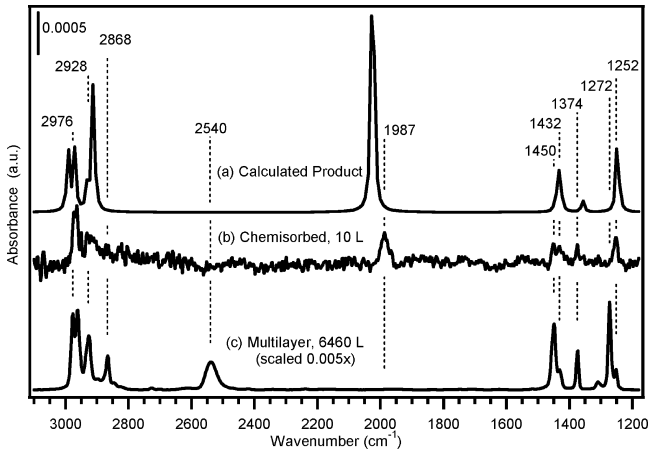


***Figure 2.*** (a) Calculated IR spectrum of the intradimer S−H dissociation product of ethanethiol across a Ge dimer of the two-dimer, intrarow $Ge_{15}H_{16}$ cluster. (b) An IR spectrum taken following a saturation exposure of ethanethiol to Ge(100)-2×1 at 310 K. (c) An IR spectrum of a multilayer of ethanethiol on Ge(100)-2×1 taken at 130 K (scaled). Geometry optimization of the product for which the IR spectrum displayed in (a) was calculated was performed with no geometric constraints.

O−H dissociated product (Figure S1 in the Supporting Information) is nearly identical to that for the intradimer adduct, hence inter- and intradimer O−H dissociated adducts cannot be experimentally distinguished from IR studies alone. On the basis of this agreement, the normal modes obtained in the DFT calculations for O−H dissociated ethanol were used to make vibrational assignments for the chemisorption spectrum.

In addition to bonds containing hydrogen, the ethanol molecule comprises a C−C−O skeleton that in principle could dissociate. However, C−C bond cleavage is not expected to occur at room temperature based on studies of related organic molecules on Ge(100)-2×1.[4,11] Less is known about O−C cleavage. It is plausible that ethanol might undergo O−C dissociation via a mechanism in which the nucleophilic "up" atom of a germanium dimer attacks the electrophilic α-carbon atom of a nearby O dative-bonded adduct. However, we can rule out this pathway based on three observations. First, it would leave the O−H group intact, and no O−H stretch is observed in the chemisorbed spectrum. Second, the appearance of a strong asymmetric C−C−O stretch peak at 1044 $cm^{-1}$ in the chemisorbed spectra confirms the presence of the C−C−O backbone at the surface. Lastly, we have calculated the energy diagram for the O−C dissociation pathway for the reaction of a related molecule, diethyl ether, discussed in Section 3.B.2. As we have shown in studies of related molecules, the energetics of bond cleavage are not significantly altered by the presence of substituents, so the energetics calculated for O−C cleavage in diethyl ether should provide reasonable guidance on the energetics for O−C cleavage in ethanol. The energy diagram calculated for O−C dissociation of diethyl ether (Figure 8) shows that O−C dissociation is kinetically prohibitive at room temperature.

Figure 2 shows (a) the calculated IR spectrum for the S−H dissociated product, (b) an IR spectrum taken following saturation exposure of ethanethiol to Ge(100)-2×1 at 310 K, and (c) an IR spectrum of a multilayer of ethanethiol on Ge(100)-2×1. The vibrational mode assignments for the major peaks are given in the Supporting Information.

There is close agreement of the multilayer spectrum in Figure 2c with previously reported IR spectra of ethanethiol in the solid phase.[33,34] Comparison of the chemisorbed ethanethiol spectrum in Figure 2b with the multilayer spectrum reveals two key changes that occur upon adsorption: (1) loss of the S−H stretch peak at 2540 $cm^{-1}$ in the multilayer and (2) growth of a Ge−H stretch peak at 1987 $cm^{-1}$. These changes indicate that the S−H bond of ethanethiol has broken, and a Ge−H bond with the surface has formed, consistent with S−H dissociation. Support for S−H dissociation is further provided by the excellent agreement between the experimental spectrum of chemisorbed ethanethiol (Figure 2b) and the IR spectrum calculated for the S−H dissociated product (Figure 2a). As with ethanol, the vibrational spectra calculated for intradimer and interdimer (Figure S2 in the Supporting Information) S−H dissociated adducts would be experimentally indistinguishable.

The possibility of C−H dissociation can be ruled out based on two pieces of evidence. First, the frequencies and relative intensities of peaks associated with C−H stretching, $CH_2$ deformation, and $CH_3$ deformation in the range of 1250−1450 $cm^{-1}$ in the multilayer spectrum are largely unchanged in the chemisorption spectrum, indicating that the $CH_2$ and $CH_3$ groups of ethanethiol molecules remain intact upon adsorption. Second, barring the unlikely event of dual S−H and C−H bond dissociation, C−H dissociation would leave an intact S−H group on the surface. Similarly, an S−C dissociation mechanism would also leave the S−H group of ethanethiol intact. However, no S−H stretch is observed in the chemisorbed spectrum, providing evidence against both C−H and S−C dissociation. Moreover, the energy diagram calculated for diethyl sulfide (a related molecule) on the Ge surface shows that S−C dissociation has a high activation barrier (Section 3.B.2). As justified earlier, we anticipate that the energetics of S−C dissociation will not be significantly altered between diethyl sulfide and ethanethiol, suggesting that the S−C dissociation of ethanethiol is kinetically prohibitive at room temperature as well.

The data collectively indicate that both ethanol and ethanethiol adsorb dissociatively on Ge(100)-2×1 at 310 K, with ethanol undergoing O−H cleavage and ethanethiol undergoing S−H dissociation. It is not possible to distinguish between intradimer and interdimer Ch−H dissociated adducts using only the IR evidence.

**2. Theoretical Ch−H Dissociation Pathways.** The observation that ethanol and ethanethiol chemisorb on Ge(100)-2×1 by Ch−H dissociation parallels the experimental and theoretical result for the room-temperature adsorption of these molecules on Si(100)-2×1.[17−20] Silvestrelli[16] used ab intio quantum simulations to predict a kinetically favorable mechanism for O−H dissociation of ethanol on Si(100), leading to the stable product observed at room temperature. Both Ge(100) and Si(100) surfaces undergo a 2×1 reconstruction, which entails the formation of tilted surface dimers composed of an electron-rich, nucleophilic "up" atom and an electron-deficient, electrophilic "down" atom.[10] Thus, it is feasible that both ethanethiol and ethanol also adsorb on Ge(100)-2×1 at 310 K via the mechanism proposed by Silvestrelli, which consists of two steps. In the first step, the chalcogen atom of the adsorbate forms a dative bond to the surface by donating a lone pair of electrons to the electrophilic down atom of the dimer. In the second and final step, the nucleophilic up atom of the same dimer abstracts a proton from the Ch atom of the adsorbed molecule. It is also

(33) Smith, D. D. *J. Mol. Spectrosc.* **1968**, *25* (2), 174.
(34) Barnes, A. J.; Howells, J. D. R.; Hallam, H. E. *J. Chem. Soc., Faraday Trans. 2* **1972**, *68* (5), 737.

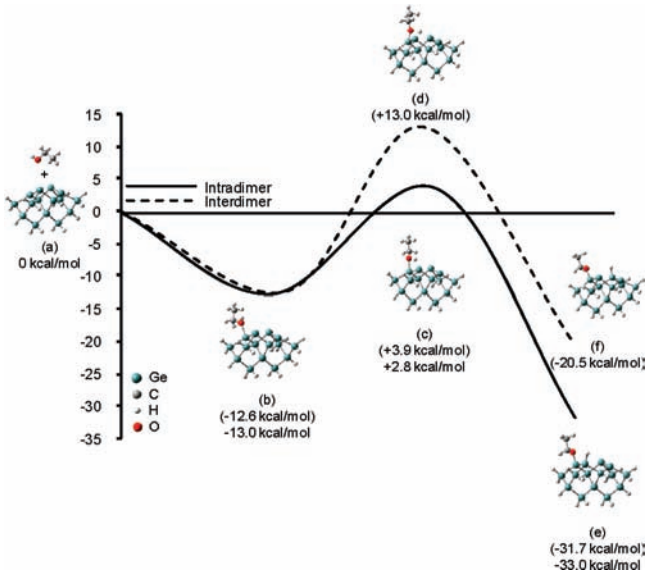


***Figure 3.*** Calculated energy diagrams for intradimer and interdimer pathways for O−H dissociation of ethanol on a $Ge_{15}H_{16}$ cluster containing two dimers within the same row. Energies are calculated with respect to the reactants (a). Critical points corresponding to the O dative-bonded state (b) and the transition states to intradimer (c) and interdimer (d) O−H dissociation. The intradimer and interdimer O−H dissociated products are denoted by (e) and (f), respectively. Energies of adducts obtained from geometry optimization using geometric constraints are shown in parentheses.

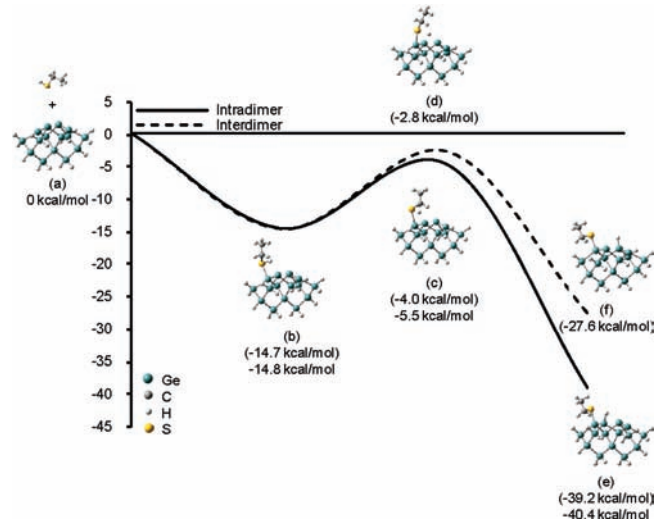


***Figure 4.*** Calculated energy diagrams for intradimer and interdimer pathways for S−H dissociation of ethanethiol on a $Ge_{15}H_{16}$ cluster containing two dimers within the same row. Energies are calculated with respect to the reactants (a). Critical points corresponding to the S dative-bonded state (b) and the transition states to intradimer (c) and interdimer (d) S−H dissociation. The intradimer and interdimer S−H dissociated products are denoted by (e) and (f), respectively. Energies of adducts obtained from geometry optimization using geometric constraints are shown in parentheses.

possible for Ch−H dissociation to proceed via an interdimer mechanism in which the nucleophilic up atom of a *neighboring* dimer abstracts the proton from the Ch atom of the adsorbed molecule.

DFT-based quantum chemical simulations were used to model both intradimer and interdimer Ch−H dissociation mechanisms for ethanol and ethanethiol on Ge(100)-2×1, which was represented by a $Ge_{15}H_{16}$ cluster containing two dimers within the same row. Though use of this cluster is not exhaustive in modeling interdimer reactions, which can proceed across two parallel dimers in the same row or across two parallel dimers in adjacent rows, it maintains a lower computational cost than a cluster containing two parallel dimers in adjacent rows while still providing a means to probe interdimer behavior. As indicated in the computational details, geometric constraints were used in optimizing adducts corresponding to points in interdimer pathways. For comparative purposes, optimization was performed for adducts in the analogous intradimer pathways using the same set of constraints. The adsorption energies extracted from calculations employing constraints, which will only be discussed in this section (3.A.2.), are enclosed in parentheses in Figures 3 and 4 to distinguish them from those extracted from calculations for which no geometric constraints were used.

Figure 3 shows the calculated energy diagrams for the intradimer and interdimer pathways for O−H dissociation of ethanol on a two-dimer, intrarow $Ge_{15}H_{16}$ cluster. The intradimer pathway is addressed first. The binding energy of the O-dative bonded precursor state is 13.0 kcal/mol. The barrier to O−H dissociation lies only 15.8 kcal/mol above the O dative-bonded state and 2.8 kcal/mol above the entrance channel, an amount almost within the uncertainty of the calculations. At room temperature, this barrier may be surmounted, especially if the ethanol molecule does not fully accommodate into the dative-bonded well. The O−H dissociated product is located 33 kcal/mol below the entrance channel, indicating the thermodynamic stability of this product. In comparing the energy values obtained with and without the use of constraints for each point shown in the intradimer pathway, it is evident that the use of the constraints does not significantly affect the energies. More significant are the differences seen between intra- and interdimer pathways. Although both the intradimer and interdimer O−H dissociation pathways lead to thermodynamically stable products, the interdimer pathway is considerably more activated, with the barrier located 13 kcal/mol above the entrance channel. We propose that the higher barrier to interdimer O−H dissociation stems from the larger mismatch between the length of the O−H bond (0.97 Å) and the interdimer Ge−Ge separation (4.3 Å); the mismatch is smaller between the O−H bond length and the intradimer Ge−Ge separation (2.5 Å). Thus, interdimer O−H dissociation requires considerably more elongation of the O−H bond. The results of the calculations suggest that only the intradimer O−H dissociated adduct should be observed at room temperature.

The intradimer and interdimer pathways for S−H dissociation of ethanethiol on the two-dimer, intrarow $Ge_{15}H_{16}$ cluster are shown in Figure 4. The barrier to intradimer S−H dissociation lies only 9.3 kcal/mol above the S dative-bonded state and is 5.5 kcal/mol *below* the entrance channel. Additionally, the intradimer S−H dissociated product is located 40.4 kcal/mol below the entrance channel, indicating that it is a thermodynamically stable product. Similar to the ethanol calculations, the use of constraints does not significantly affect the energies for ethanethiol (Figure 4). Some differences are, however, seen between the intradimer and interdimer S−H dissociation pathways. The interdimer product is ∼12 kcal/mol less thermodynamically favorable than the intradimer product, although both products are thermodynamically stable. Both pathways also possess a small activation energy differing by only ∼1 kcal/mol. Consequently, unlike ethanol, for which the kinetics should favor primarily intradimer Ch−H dissociation, the corresponding

***Scheme 1.*** Overall Chemical Reaction for Ch−H Dissociation across a Ge Dimer[a]

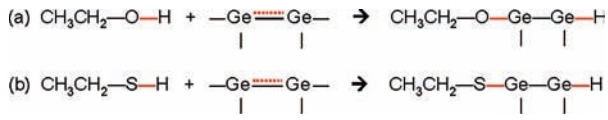

[a] (a) O−H dissociation of ethanol. (b) S−H dissociation of ethanethiol.

reaction with ethanethiol should lead to both intradimer and interdimer Ch−H dissociated adducts.

For both ethanol and ethanethiol, the DFT calculations support the IR findings, which indicate that the Ch−H dissociation reaction occurs on Ge(100)-2×1 to form stable products at room temperature. However, a more in depth comparison of the critical points and product states of these pathways provides insight into differences between the two molecules. As seen in Figures 3 and 4, the S−Ge dative bond of the ethanethiol adduct (14.8 kcal/mol) is slightly stronger (by 1.8 kcal/mol) than the O−Ge dative bond of the ethanol adduct (13.0 kcal/mol). However, unlike the dative bond energies, the energetics of the subsequent Ch−H dissociations are notably different. Comparison of the two intradimer or two interdimer pathways reveals that the barrier to O−H dissociation is almost twice that to S−H dissociation from the respective dative bonded states, and the S−H dissociation reaction is ∼7 kcal/mol more exothermic than the corresponding O−H dissociation reaction. Consequently, the S−H dissociation reaction is both kinetically and thermodynamically more favorable than the corresponding O−H dissociation reaction−a trend opposite to that for reaction of these molecules on Si(100)-2×1.[20,21,35]

**3. Bond Energy Calculations.** To understand why the S−H dissociation pathway is more exothermic than the O−H dissociation pathway on germanium, DFT-based quantum chemical simulations were used to perform bond energy calculations for bonds broken or formed during the Ch−H dissociation reactions of ethanethiol and ethanol on the Ge(100)-2×1 surface. Scheme 1 displays these reactions, with the bonds broken or formed highlighted in red. The germanium surface is represented by a germanium dimer, the fundamental reactive unit in these reactions.

Quantitatively, the difference in exothermicity of these reactions is given by $\Delta(\Delta H_{rxn})$, where

$$\Delta(\Delta H_{rxn}) = (BE_{O-H} - BE_{O-Ge}) - (BE_{S-H} - BE_{S-Ge}) \quad (1)$$

and BE refers to the positive bond energy. Note that in determining the *difference* in exothermicity between reactions a and b, bonds broken or formed in *both* reactions (e.g., Ge−Ge or Ge−H) can be neglected. As described in Experimental and Computational Details, the bond energy calculations employed a small $Ge(GeH_3)_3$ fragment to represent the germanium surface. The calculated bond energies, together with analogous energies for silicon, are displayed in Table 1.

Where experimental data are available, the calculated bond energies are found to be in good agreement with the literature. Specifically, the experimentally determined S−H and O−H bond energies of ethanethiol and ethanol, respectively, are 87.3 and 105.4 kcal/mol, [36] values that agree to within 10% of the energies calculated here. Using the calculated bond energies, the resulting value for $\Delta(\Delta H_{rxn})$ is 6.5 kcal/mol on Ge. This result is within 1 kcal/mol of the value obtained using the *relative* interdimer (7.1 kcal/mol) or intradimer (7.4 kcal/mol) product energies from Figures 3 and 4 based on calculations using the more accurate two-dimer cluster, thus further supporting the accuracy of these calculated bond energies.

***Table 1.*** Bond Energies for Bonds Broken or Formed during the Ch−H Dissociation Reactions of Ethanol and Ethanethiol on the Ge(100)-2×1 and Si(100)-2×1 Surfaces[a]

| bond | energy (BE), kcal/mol |
|---|---|
| O−H | 97.0 |
| S−H | 81.4 |
| O−Ge | 68.5 |
| S−Ge | 59.4 |
| O−Si | 84.0 |
| S−Si | 64.7 |

[a] Here bond energy is defined as the energy required to break a bond and, thus, has a positive value.

The source of this result can be understood by considering the calculated values for the bond energies of which $\Delta(\Delta H_{rxn})$ is comprised. According to Table 1, the O−Ge bond which forms in the reaction is stronger than the S−Ge bond by 9.1 kcal/mol. However, the O−H bond, which must be broken, is stronger than the S−H bond by 15.6 kcal/mol. Therefore, the amount by which the O−Ge bond is stronger than the S−Ge bond (9.1 kcal/mol) is much smaller than the amount by which the O−H bond is stronger than the S−H bond (15.6 kcal/mol), thus yielding the overall result of O−H dissociation on Ge(100)-2×1 being less thermodynamically favorable than the corresponding S−H dissociation. In other words, the S−H dissociation reaction on Ge(100)-2×1 is thermodynamically more favorable than the corresponding O−H dissociation reaction not because of the strength of the S−Ge bond relative to that of the O−Ge bond but rather because of the weakness of the S−H bond relative to that of the O−H bond.

Both the kinetics and thermodynamics favor S−H dissociation over O−H dissociation on Ge. Interestingly, this difference is reversed on Si. On Si, experiments have shown that methanol undergoes O−H dissociation on Si(100)-2×1 at 150 K,[21] whereas S−H dissociation of methanethiol does not occur until 170 K,[20] indicating that the reaction barrier is smaller for O−H dissociation. Moreoever, our bond energy calculations (see Table 1) carried out for Ch−H dissociation of ethanol and ethanethiol on Si show that O−H dissociation is 3.7 kcal/mol more exothermic than S−H dissociation. The bond energy calculations further indicate that the thermodynamic favorability of O−H dissociation over S−H dissociation on Si is dominated by the significantly greater strength of the O−Si bond versus that of the S−Si bond.

**B. Diethyl Ether versus Diethyl Sulfide.** In the previous sections, the mechanism for intradimer Ch−H dissociation of ethanol and ethanethiol on Ge(100)-2×1 was shown to proceed through a Ch−Ge dative-bonded precursor state. In this section, diethyl ether and diethyl sulfide adsorption on Ge(100)-2×1 are studied to experimentally measure O−Ge and S−Ge dative bond strengths. Based on the ethanol and ethanethiol results discussed in earlier sections and on previous adsorption studies of related molecules on Ge(100)-2×1 and Si(100)-2×1, adsorption mechanisms that break bonds within these molecules (C−H, C−C, and Ch−C) are not likely to occur at room temperature.[17−20,37,38] Consequently, each molecule likely reacts with the surface via dative bonding through the Ch atom. Since these dative bonds are weaker than the bonds present in the adsorbates, first-order molecular desorption of these molecules from the surface is

(35) Edamoto, K.; Kubota, Y.; Onchi, M.; Nishijima, M. *Surf. Sci.* **1984**, *146* (1), L533.
(36) *CRC Handbook of Chemistry and Physics*, 89th ed.; Taylor and Francis: Boca Raton, FL, 2008.

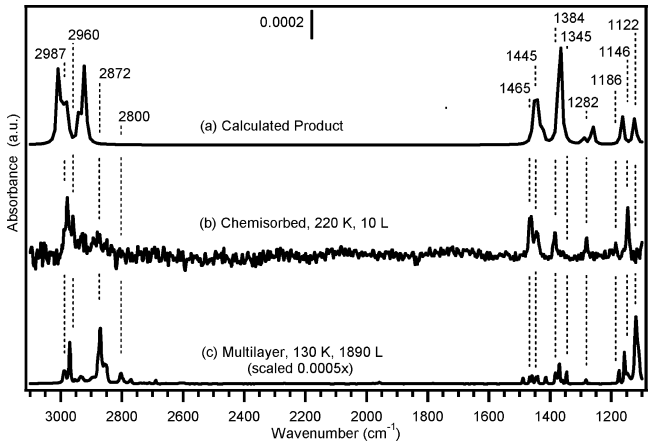


***Figure 5.*** (a) Calculated IR spectrum of diethyl ether O dative-bonded to the down atom of a Ge dimer of the two-dimer, intrarow $Ge_{15}H_{16}$ cluster. (b) IR spectrum taken following saturation exposure of diethyl ether to Ge(100)-2×1 at 220 K. (c) An IR spectrum of a multilayer of diethyl ether on Ge(100)-2×1 taken at 130 K (intensity scaled).

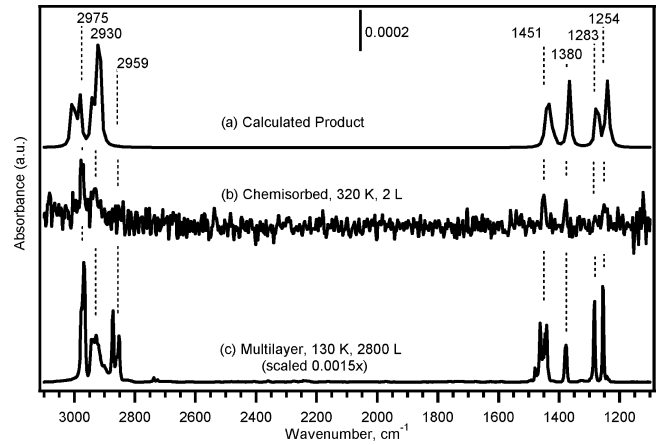


***Figure 6.*** (a) Calculated IR spectrum of diethyl sulfide S dative-bonded to the down atom of a Ge dimer of the two-dimer, intrarow $Ge_{15}H_{16}$ cluster. (b) IR spectra taken following saturation exposure of diethyl sulfide to Ge(100)-2×1 at 320 K. (c) An IR spectrum of a multilayer of diethyl sulfide on Ge(100)-2×1 taken at 130 K (intensity scaled).

expected upon heating. In this case, IR spectra of the temperature-dependent adsorption of diethyl ether and diethyl sulfide can be used to evaluate O−Ge and S−Ge dative bond strengths, respectively.

**1. IR Analysis.** Figure 5 shows (a) the calculated IR spectrum for the O dative-bonded diethyl ether adduct, (b) an IR spectrum taken following saturation exposure of 10 L of diethyl ether at 220 K, and (c) an IR spectrum of a multilayer of diethyl ether on Ge(100)-2×1. The vibrational assignments for labeled peaks in the experimental spectra of Figure 5 are included in the Supporting Information. The multilayer spectrum in Figure 5c agrees well with previously reported IR spectra of diethyl ether in the solid phase,[39−41] and vibrational assignments for the multilayer were made using this literature as well as that of IR spectra of diethyl ether in the liquid and vapor phases.[42]

The chemisorbed spectrum (Figure 5b) closely matches the calculated IR spectrum of the O dative-bonded surface adduct (Figure 5a). We note that the spectrum also agrees, though to a lesser extent, with the calculated IR spectrum of an O−C dissociated surface adduct (Figure S3 in Supporting Information). Hence, IR spectroscopy alone cannot be used to rule out O−C dissociation. However, as will be shown below, a large activation barrier makes O−C dissociation kinetically prohibitive for the range of temperatures probed, supporting the assignment of the product as an O dative-bonded species. In addition, the absence of a Ge−H stretch in the chemisorbed spectrum indicates that no C−H dissociation is occurring. IR spectra were also collected following saturation exposures of diethyl ether at surface temperatures of 250, 260, and 270 K. The peak positions and relative intensities of the chemisorbed spectra taken at these temperatures match those of the spectrum taken at 220 K, suggesting that the surface product is the same over the temperature range of 220−270 K. However, the overall intensities are reduced with increasing temperature. These observations collectively suggest that molecular desorption rather than decomposition occurs upon heating.

Figure 6 shows (a) the calculated IR spectrum for the S dative-bonded diethyl sulfide adduct, (b) an IR spectrum taken following saturation exposure of 100 L of diethyl sulfide to Ge(100)-2×1 at 320 K, and (c) an IR spectrum of a multilayer of diethyl sulfide. The multilayer spectrum agrees well with previously reported IR spectra of diethyl sulfide in the solid phase,[43,44] and vibrational assignments (see Supporting Information) for the multilayer were made using this literature. The chemisorbed spectrum (Figure 6b) agrees with the calculated IR spectra of both the S dative-bonded (Figure 6a) and S−C dissociated (Figure S4 in Supporting Information) surface adducts. Again, the theoretical calculations described below reveal a large activation barrier for S−C dissociation, indicating that for the range of temperatures probed, S−C dissociation is kinetically prohibitive and should not be observed. Lastly, no Ge−H stretch is present in these chemisorbed spectra, indicating that C−H dissociation does not occur. Consequently, diethyl sulfide, like diethyl ether, reacts with the Ge(100)-2×1 surface via Ch dative bonding.

IR spectra collected after exposure of diethyl sulfide at surface temperatures of 250, 280, 310, 330, 340, and 350 K (not shown) reveal no significant shifts in peak positions or changes in relative intensities, suggesting that the same surface adduct is present between 250 and 350 K. As the temperature increases over this range, the peaks attenuate in concert and no new peaks appear. This result is attributed to molecular desorption of the product from the surface.

The average surface coverage, $\bar{\theta}$, of the adsorbate during an isothermal IR measurement, which averages 1000 scans taken over the duration of the process, can be approximated by the integrated IR peak intensity over several vibrational modes. Figure 7 shows the normalized average IR peak area as a function of temperature for both diethyl ether and diethyl sulfide. The decrease in IR peak area as temperature is increased corresponds to molecular desorption of the adsorbate. It is clear from Figure 7 that diethyl sulfide desorbs at a higher temperature than does diethyl ether. Assuming first-order desorption kinetics, we can determine the binding energy of each of the adsorbates

(37) Coulter, S. K.; Schwartz, M. P.; Hamers, R. J. *J. Phys. Chem. B* **2001**, *105* (15), 3079.
(38) Zhu, Z. M.; Srivastava, A.; Osgood, R. M. *J. Phys. Chem. B* **2003**, *107* (50), 13939.
(39) Snyder, R. G.; Zerbi, G. *Spectrochim. Acta, Part A* **1967**, *23* (2), 391.
(40) Cook, J. J. *Surf. Sci.* **1996**, *365* (3), 573.
(41) Perchard, J. P. J. *Spectrochim. Acta, Part A* **1971**, *27* (3), 447.
(42) Wieser, H. H. *Spectrochim. Acta, Part A* **1968**, *24* (8), 1055.
(43) Cataliotti, R. R. *Can. J. Phys.* **1986**, *64* (1), 100.
(44) Ohsaku, M. M. *Bull. Chem. Soc. Jpn.* **1972**, *45* (3), 956.
(45) Redhead, P. A. *Vacuum* **1962**, *12* (4), 203.

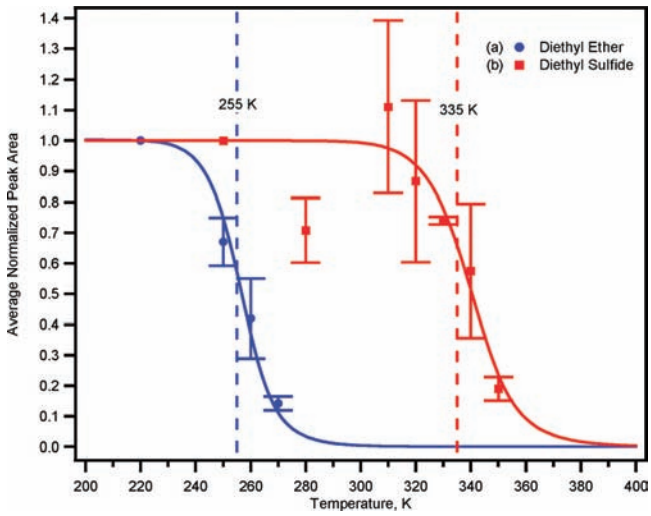


***Figure 7.*** Average normalized IR peak area versus temperature for (a) diethyl ether and (b) diethyl sulfide on Ge(100)-2×1. For each data point, the area of each peak in the chemisorbed spectrum is normalized to its value at the lowest substrate temperature. The normalized peak areas are then averaged, and the result is plotted against the substrate temperature with error bars indicating the standard deviation. Each data set was fit to $\bar{\theta}(T)/\bar{\theta}(T_{min})$ using eq 4, as shown by the solid curves.

from this plot. The desorption rate expression for first-order desorption kinetics is given by

$$\text{desorption rate} = -\frac{d\theta}{dt} = k_o\theta \exp\left(\frac{-\Delta E}{RT}\right) \qquad (2)$$

where $\theta$ = surface coverage, $t$ = time, $k_0$ is the pre-exponential factor, $\Delta E$ = dative bond strength, $R$ = the universal gas constant, and $T$ = temperature.

Solving eq 2 for $\theta$ at time $t$ yields

$$\theta = \theta_0 \exp\left[-k_o t \exp\left[\frac{-\Delta E}{RT}\right]\right] \qquad (3)$$

where $\theta_o$ is the initial saturation coverage. To account for the contribution from desorption that occurs over the duration of the IR scanning process, we calculate an average surface coverage, $\bar{\theta}$, from time $t$= 0 to time $t = t_s$ (at the end of the scanning process) by integrating eq 3 and dividing by the measurement time, $t_s$. This yields eq 4

$$\bar{\theta} = \frac{\theta_0 \exp\left[\frac{\Delta E}{RT}\right]\left[1 - \exp\left[-k_0 t_s \exp\left[\frac{-\Delta E}{RT}\right]\right]\right]}{k_0 t_s} \qquad (4)$$

To normalize the data in Figure 7, each integrated IR peak intensity evaluated at T was ratioed to the corresponding value at the lowest temperature probed, $T_{min}$, for diethyl ether and diethyl sulfide. Therefore, the data in Figure 7 was fit to $\bar{\theta}(T)/\bar{\theta}(T_{min})$, evaluated using eq 4 with $t_s$ = 300 s (the approximated length of an isothermal IR scan in these experiments), $k_0 = 10^{13}$ s$^{-1}$ (a pre-exponential factor value commonly used for molecular desorption rates[13,45]), $T_{min,\ ether}$ = 220 K, and $T_{min,\ sulfide}$ = 250 K. The fit allows us to solve for $\Delta E$, which is assumed to be constant.

Figure 7 shows the result of this fit for both diethyl sulfide and diethyl ether. Using this procedure, the dative bond strengths of diethyl ether/Ge(100)-2×1 and diethyl sulfide/Ge(100)-2×1 are estimated to be 17.9 and 23.8 kcal/mol, respectively. The values extracted from the isothermal IR experiments therefore indicate that the S−Ge dative bond of diethyl sulfide is stronger than the O−Ge dative bond of diethyl ether by 5.9 kcal/mol.

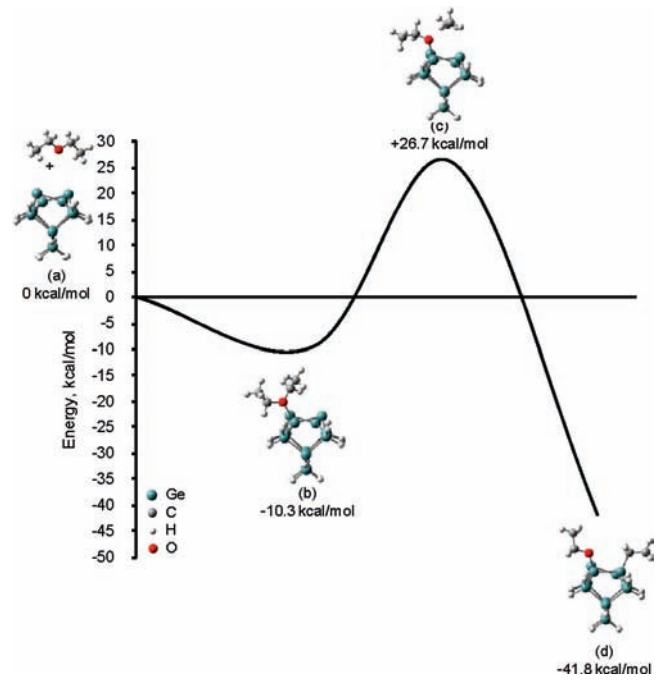


***Figure 8.*** Calculated energy diagram for intradimer O−C dissociation of diethyl ether on a $Ge_{15}H_{16}$ cluster containing two dimers within the same row. Energies are calculated with respect to the reactants (a). Critical points corresponding to the O dative-bonded state and the transition state to O−C dissociation are indicated by (b) and (c), respectively. The O−C dissociated product is denoted by (d).

Using the dative bond strength values, the temperature at which the desorption rate is a maximum can be determined from eq 3 to estimate the temperature stability of these adsorbate systems. The maximum desorption rate occurs when $d^2\theta/dT^2 = 0$. Therefore, the desorption temperatures for the diethyl ether and diethyl sulfide systems, indicated by the dashed lines in Figure 7, show that these systems are stable up to 255 and 335 K, respectively.

**2. Calculated Ch−C Dissociation Pathways.** To better understand the adsorption process at the surface, we have calculated pathways for intradimer Ch−C dissociation of diethyl sulfide and diethyl ether on the $Ge_{15}H_{16}$ cluster. These pathways are shown in Figures 8 and 9, respectively.

A comparison of the Ch dative-bonded states of these calculated pathways shows that the S−Ge dative bond of the diethyl sulfide adduct is 7.7 kcal/mol more stable than the O−Ge bond of the corresponding diethyl ether adduct. This difference in binding energies supports the experimental data presented for the diethyl ether and diethyl sulfide systems, which indicated that the S−Ge dative bond of the diethyl sulfide adduct is stronger than the O−Ge dative bond of diethyl ether adduct by approximately the same amount (5.9 kcal/mol).

In examining the S−C and O−C dissociation pathways, it is apparent that both Ch−C dissociated products are thermodynamically stable and are favored over the corresponding Ch dative-bonded products: The O−C dissociated ether and the S−C dissociated sulfide products are 41.8 and 45.7 kcal/mol below the entrance channel, respectively. However, both dissociation pathways are highly activated kinetically. The transition state to O−C dissociation of diethyl ether is 37.0 kcal/mol above the O dative-bonded precursor state and 26.7 kcal/mol above the entrance channel. Similarly, the transition state to S−C dissociation of diethyl sulfide is located far above the

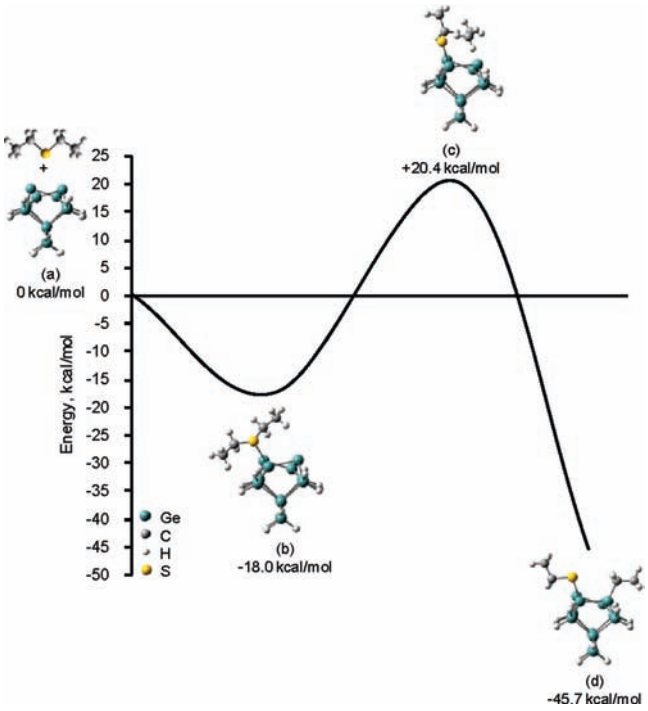


***Figure 9.*** Calculated energy diagram for intradimer S−C dissociation of diethyl sulfide on a $Ge_{15}H_{16}$ cluster containing two dimers within the same row. Energies are calculated with respect to the reactants (a). Critical points corresponding to the S dative-bonded state and the transition state to S−C dissociation are indicated by (b) and (c), respectively. The S−C dissociated product is denoted by (d).

S dative-bonded precursor state and the entrance channel (by 38.4 and 20.4 kcal/mol, respectively). Consequently, although S−C dissociation of diethyl sulfide and O−C dissociation of diethyl ether lead to products which are thermodynamically stable and favored over the corresponding Ch dative-bonded products, the high barriers to these dissociations suggest that both S−C and O−C dissociation pathways will be kinetically prohibitive for the range of temperatures probed, as consistent with the IR findings.

To examine the trend in Ge dative bond strength along Group VI elements, we also calculated the Se−Ge dative bond strength for diethyl selenide dative-bonded through the Se atom to the $Ge_{15}H_{16}$ Ge cluster. This calculation, in conjunction with the analogous calculations for the sulfide and the ether, show that the Se−Ge bond (19.4 kcal/mol) is stronger than the S−Ge bond (18.0 kcal/mol). Consequently, Ch−Ge dative covalent bond strength appears to increase down Group VI. However, the Se−Ge dative bond is stronger than the S−Ge dative bond by only small amount (1.4 kcal/mol). Bond energy calculations were also performed to evaluate the strength of an ordinary covalent Se−Ge bond between $SeCH_2CH_3$ and $Ge(GeH_3)_3$ fragments. This calculation shows that the covalent Se−Ge bond (56.9 kcal/mol) is slightly weaker (by 2.5 kcal/mol) than the S−Ge bond (59.4 kcal/mol), and 11.6 kcal/mol weaker than the O−Ge bond (68.5 kcal/mol). Consequently, *ordinary* covalent Ch−Ge bond strength *decreases* down Group VI, a trend opposite to that for *dative* covalent Ch−Ge bond strength.

## 4. Discussion

The study of the adsorption of chalcogen-containing molecules at the Ge(100)-2×1 surface reveals interesting trends in bond strengths. Namely, the trend in bond strength for ordinary covalent bonds to Ge in going from O to Se is *opposite* to that for dative bonds. The DFT bond energy calculations show that the strength of ordinary covalent Ch−Ge bonds *decreases* down Group VI, whereas the calculations, supported by IR spectroscopic data for O- and S-containing molecules, show that the strength of dative covalent Ch−Ge bonds *increases* down Group VI.

Quantum mechanically, the strength of a bond depends upon the overlap, exchange, and Coulomb integrals. As will be shown below, the extent of overlap between the orbitals that combine to form the bond is a primary factor affecting bond strength. This overlap integral depends upon the nature of the orbitals (e.g., the size and symmetry of the orbitals), as well as the relative energies of the combining orbitals. The bonding is in turn influenced by properties such as electronegativity of the atoms, steric effects of the molecule, and inductive effects of substituents.

The decrease in ordinary covalent Ch−Ge bond strength down Group VI of the periodic table is consistent with the expected trend in atomic properties down this group. Two important atomic properties that affect covalent bond strength are orbital size and electronegativity. The covalent Ch−Ge bond between the adsorbate and the germanium surface is formed by overlap primarily between one of the degenerate LUMOs of the germanium surface and the HOMO of the adsorbate, as indicated by the molecular orbital surfaces derived from the DFT calculations. The LUMOs of the germanium surface are localized on electron-deficient down atoms of germanium dimers and resemble valence p orbitals of a Ge atom. The HOMO of the adsorbates, which is occupied by a lone pair of electrons, resembles the valence p orbitals of the Ch atom on which it is localized. However, as one moves down Group VI, the regions of highest electron density in the HOMO extend further from the nucleus. For example, for the selenium-, sulfur-, and oxygen-containing adsorbates, the HOMO arises from a 4p orbital on Se, a 3p orbital on S and a 2p orbital on O, respectively. As a result of the larger orbitals, Ch−Ge bond length increases down Group VI. For example, the DFT calculations show that upon dissociative adsorption of ethanethiol and ethanol at the germanium surface, the S−Ge and O−Ge bond lengths are 2.54 and 1.82 A, respectively. The longer bond lengths are accompanied by reduced orbital overlap between S and Ge atoms, corresponding to a weaker covalent S−Ge bond compared to the O−Ge bond.

Another factor reducing ordinary covalent Ch−Ge bond strength down Group VI is electronegativity. The strength of ordinary covalent bonds is dependent upon the relative electronegativities of the atoms forming the bond.[46] For the chalcogenides, electronegativity decreases with increasing atomic number down Group VI. The Pauling electronegativities of Ge, O, S, and Se atoms are 2.01, 3.44, 2.58, and 2.55, respectively.[46] Consequently, the difference in Pauling electronegativity between oxygen and germanium (1.43) is almost three times as large as either that between sulfur and germanium (0.57) or that between selenium and germanium (0.54). This trend favors a decrease in ordinary covalent Ch−Ge bond strength down Group VI. Consequently, both the poorer orbital overlap and lower electronegativity difference lead to a decrease in ordinary covalent Ch−Ge bond strength down Group VI.

Interestingly, although the O−Ge bond is stronger than the S−Ge bond, the overall exoenergicity of the Ch−H dissociation

(46) Pauling, L. *J. Am. Chem. Soc.* **1932**, *54*, 3570.

reaction at the Ge(100)-2×1 surface in which a Ch−Ge bond is formed is greater for S−H dissociation (see Figures 3 and 4). The bond energy calculations show clearly that the origin of this higher exoenergicity is the weakness of the S−H bond compared to the O−H bond. Just as for the covalent bonds with Ge, the S−H bond is weaker than the O−H bond because of the larger S 3p orbital and the smaller electronegativity difference with H. Moreover, the relative strength of the Ch−H bond is reflected in the activation barrier for the Ch−H dissociation reactions shown in Figures 3 and 4. From the dative-bonded precursor state, the activation barrier for O−H dissociation is approximately twice that for the S−H dissociation reaction. The Ch−H bond is stretched at the transition state, and the energy required to do this is lower for the weaker S−H bond. This supposition is supported by the transition state calculations carried out for the intradimer reaction, which show the following. At the transition state, the S−H bond is stretched 22% compared to the S−H bond length in the dative-bonded thiol, whereas the O−H bond is stretched by almost twice that amount (39%) relative to the O−H bond length in the dative-bonded alcohol. At the same time, the Ge−H bond at the transition state to S−H dissociation is 25% longer than the Ge−H bond in the S−H dissociated product, while the Ge−H bond at the transition state to O−H dissociation is 16% longer than the Ge−H bond in the O−H dissociated product. These values suggest that the transition state for S−H dissociation occurs relatively earlier in the pathway as compared to the occurrence of the transition state in the O−H dissociation pathway.

We now turn to an explanation for why the observed periodic trend in bond strength is opposite for dative Ch−Ge bonds; namely, dative covalent Ch−Ge bond strength increases down Group VI. The difference is clearly evident in the thermal annealing studies in which the dative-bonded diethyl sulfide desorbs from the surface at a temperature almost 80 K higher than does the dative-bonded diethyl ether, corresponding to a dative bond 5.9 kcal/mol stronger, as calculated by kinetic analysis of integrated IR peak intensity data obtained at different substrate temperatures. This is supported by the DFT calculations, which show the sulfide forms a dative bond 7.7 kcal/mol stronger than that formed by the ether.

The explanation for this difference is that unlike with the ordinary covalent bonds, for which the periodic properties of orbital size and electronegativity both worked *in concert* to favor a higher bond strength for the lighter chalgogenide, these properties exert *opposite* effects on dative bond strength. As with the ordinary covalent bond, the orbital on the molecule involved in formation of the dative bond is the HOMO, which resembles the valence p orbitals of the Ch atom on which it is localized. This orbital is occupied by a lone pair of electrons, which donate electron density to the electrophilic Ge surface atom. Down Group VI, the increase in HOMO orbital size should reduce orbital overlap with a degenerate LUMO of the Ge surface, leading to a reduction in Ch−Ge bond strength down the group. However, electronegativity favors dative bonding by the least electronegative Ch atom. The reason for this effect is that in a dative bond, the electron donor provides both of the electrons. Consequently, dative bond formation is largely dependent on the properties of the charge donating atom, which is the Ch atom of the adsorbate. Since a more electronegative Ch atom is less able to share electrons with other atoms and the Ch atom incurs a partial positive charge upon dative bond formation, it follows that dative bond strength is inversely proportional to the electronegativity of the donating atom. Oxygen (Pauling electronegativity of 3.44) is much more electronegative than sulfur (2.58), which, in turn, is slightly more electronegative than selenium (2.55). This suggests that if other effects were unimportant, selenium would form the strongest dative bonds with the germanium surface, followed by sulfur and then oxygen, as found in this study. The effect of electronegativity, thus, apparently dominates the relative dative bond strength for this system.

Although the sulfur dative bonds are stronger than the oxygen dative bonds, the DFT calculations indicate that this difference is much more pronounced for the sulfide/ether system than for the thiol/alcohol system. The calculations show the sulfide forms a dative bond 7.7 kcal/mol stronger than the ether. Yet the S-dative bond of ethanethiol is calculated to be only 1.8 kcal/mol stronger than the O-dative bond of ethanol. Although we are not certain of the origin of this difference, we can discuss possible causes. Structurally, the difference between these two sets of molecules is the presence of an additional ethyl substituent in place of hydrogen. This ethyl substituent will have at least two effects: inductive and steric. An ethyl group is more electron donating than hydrogen, which by increasing the electron density on the Ch atom should have a tendency to increase dative bond strength. On the other hand, the ethyl group is bulkier than a hydrogen atom, increasing the steric effect. The HOMO surfaces of the R−Ch−R and R−Ch−H adsorbates (Ch = O, S only) calculated using DFT and representative of the lone pairs of electrons on the Ch atoms indicate that the increase in inductive effect upon substitution (and, hence, increase in Ch−Ge bond strength) is significant for the sulfur-containing molecule. DFT calculations show that substituting an ethyl group for the hydrogen bound to the S atom of the S dative-bonded ethanethiol adduct increases S−Ge bond strength by 3.2 kcal/mol (Figure 4 vs Figure 9). Conversely, the analogous substitution on the O-dative bonded ethanol adduct *decreases* O−Ge bond strength by 2.7 kcal mol, indicating that the steric effects likely dominate for the O-containing adduct. (Figure 3 vs Figure 8).

## 5. Conclusions

We have investigated the behavior of sulfur- versus oxygen-containing organic molecules at the Ge(100)-2×1 surface under UHV conditions using MIR-IR spectroscopy and DFT to better understand the relative success of sulfur over oxygen in germanium passivation and the detailed bonding of these atoms at the surface.

The IR results show that ethanol and ethanethiol both adsorb via Ch−H dissociation at 310 K. This finding is supported by DFT calculations, which reveal that both pathways are kinetically accessible via a Ch dative-bonded precursor state that is followed by Ch−H dissociation, which leads to thermodynamically stable products. The theoretical results further indicate that of the two Ch−H dissociations, S−H dissociation is both kinetically and thermodynamically more favorable. Thermodynamic insight into the origin of this result was supplied by DFT bond energy calculations of bonds broken or formed in each Ch−H dissociation. These results show that S−H dissociation is more favorable than O−H dissociation because, contrary to the trend on silicon, the difference in thermodynamics on Ge(100) is dominated by the difference in S−H and O−H bond strengths, thus rendering S−H dissociation more energetically favorable.

The study of ether and sulfide functional groups provides a means to experimentally probe Ch−Ge dative-bonded precursor states. IR results show that diethyl ether and diethyl sulfide both adsorb via Ch dative bonding for temperatures up to approximately 255 and 335 K, respectively, above which the dative-bonded molecules molecularly desorb. The desorption temperatures, which are a function of Ch−Ge dative bond strength, show that the S−Ge dative bond of a sulfide is 5.9 kcal/mol stronger than the O−Ge dative bond of an ether. This trend is consistent with that predicted by DFT calculations.

A comparison of Ch−Ge bond energies across oxygen, sulfur, and selenium obtained by DFT calculations shows that whereas Ch−Ge dative bond strength *increases* down Group VI, Ch−Ge ordinary covalent bond strength *decreases* down Group VI. The opposite trends are attributed to the different role that electronegativity plays in affecting the orbital overlap in dative versus ordinary covalent bonds. In both types of bond, orbital overlap between the Ch HOMO and the Ge LUMO is reduced down Group VI because the size of the Ch orbital increases. In the case of ordinary covalent bonds, bond strength is enhanced by the difference in electronegativity between the Ch and Ge atoms, thus reinforcing the effects of orbital overlap and rendering the O−Ge bond the strongest ordinary covalent Ch−Ge bond. On the other hand, there is an *inverse* relationship between dative bond strength and electronegativity of the charge-donating atom, with more electronegative atoms being poorer charge donors. This effect of electronegativity dominates the stabilizing effect of orbital overlap for Ch−Ge dative bonds, leading to the strongest bonding by the heavier Group VI atoms. Lastly, for the range of functional groups probed across S- and O-containing adsorbates, the magnitude of the strength of S−Ge dative bonds over O−Ge dative bonds increases with substitution of bulkier groups on the Ch atom of the adsorbate.

**Acknowledgment.** This work was supported by the National Science Foundation (CHE 0615087). Scientific discussions with Dr. Charles B. Musgrave and Paul W. Loscutoff were also greatly appreciated.

**Supporting Information Available:** Mode assignments for peaks in the chemisorbed and multilayer IR spectra for each adsorbate/Ge(100)-2×1 system probed (Tables S1−S5), calculated IR spectra of interdimer Ch−H dissociated adducts for ethanol (Figure S1) and ethanethiol (Figure S2), calculated IR spectra of intradimer Ch−C dissociated adducts for diethyl ether (Figure S3) and diethyl sulfide (Figure S4), and complete ref 22. This material is available free of charge via the Internet at http://pubs.acs.org.

JA808066T